Catalysis Today 150 (2010) 255–263

Contents lists available at ScienceDirect

Catalysis Today

journal homepage: www.elsevier.com/locate/cattod

Reactivity study of Athabasca vacuum residue in hydroconversion conditions

P. Danial-Fortain [a,b], T. Gauthier [a,*], I. Merdrignac [a], H. Budzinski [b]

[a] IFP-Lyon, Rond-point de l'échangeur de Solaize, BP 3, 69360 Solaize, France
[b] Université Bordeaux1, ISM-LPTC, UMR CNRS 5255, 351, Cours de la Libération, 33405 Talence, France

ARTICLE INFO

Article history:
Available online 7 November 2009

Keywords:
Hydroconversion
Ebullated bed
SARA
Reactivity

ABSTRACT

Hydroconversion reactivity of an Athabasca vacuum residue (VR) has been studied in a batch autoclave reactor, as part of a work dedicated to the study of detailed hydroconversion mechanisms. In this work, as a first step, a detailed analytical study was performed on several vacuum residues. Saturates, Aromatics, Resins and Asphaltenes (SARA) composition strongly varies for different feeds, but SAR fractions analyses show strong similarities (^{13}C NMR distribution and molecular weight). Therefore, SARA compositions may explain feed hydroconversion differences.

The reactivity of the whole Athabasca vacuum residue has been studied under deep hydroconversion conditions in a batch autoclave. Process severity was adjusted varying by temperature from 395 up to 420 °C. Catalytic effect was also evaluated. As expected, results show that VR conversion increases with temperature. Product yields were obtained and depend mostly on residue conversion. The results also confirm that cracking reaction mechanisms are initiated thermally and that radicals formed are stabilized by catalytic hydrogenation.

In order to better understand feedstock effects on reactivity, we have also conducted a dedicated study in order to separate the Athabasca vacuum residue in different families, each of them containing mainly asphaltenes, resins or an aromatics/saturates mixture. The reactivity of those cuts will be studied in a next step to highlight feed composition effects.

1. Introduction

Nowadays, the heavy fuel oil demand decreases, while at the same time, there is an increasing demand for motor fuels. With the conventional crude oil production declining and being replaced by heavier feedstocks such as bitumen, more and more petroleum residues have to be converted into lighter fractions.

Residue of heavy crude oils can be upgraded through various existing processes [1,2]. One of the challenges to face while upgrading residues is to handle properly the asphaltenes contained in the feed [3]. Different available strategies to handle upgrading of heavy residue feedstocks containing asphaltenes can be proposed: asphaltenes can either be removed from the residue feedstock or converted. Asphaltene removal is industrially carried out through Solvent DeAsphalting (liquid–liquid extraction) producing asphalts on one side and deasphalted oil on the other side, or through coking processes (thermal cracking where asphaltene molecules are converted into coke). However, it is also possible to consider asphaltene conversion into valuable hydrocarbons. This requires severe operating conditions at high temperature and hydrogen partial pressure while using a hydrogenation catalyst with low-acidic support in order to avoid high coke formation. High asphaltene hydroconversion levels are achievable in these conditions and the yield of liquid produced by such processes is much higher than with asphaltene removal processes. The high metal content of feeds containing asphaltenes as well as the control of reaction exothermicity impose to operate residue hydroconversion processes with specific technologies such as ebullated bed or slurry technology [3–5]. Indeed, metals such as nickel and vanadium are concentrated in residue feeds and will progressively deposit and concentrate on the hydroconversion catalyst. Catalyst addition is then required to maintain catalyst activity during the operation. Furthermore, conversion mechanisms combined with subsequent hydrogenation generate significant reaction heat that needs to be controlled by an adequate mixing in order to avoid large thermal gradients along the reactor.

Hydroconversion processes are commercially available to handle upgrading of heavy residue feedstocks. Ebullated beds are used to convert atmospheric or vacuum residues at high temperature (up to 450 °C) and Liquid Hourly Space Velocity (LHSV) in the range of 0.15–1.3 h^{-1}, with a low-acidic support hydrogenation catalyst in order to minimize coke deposit. High residue hydroconversion levels are achievable in these conditions but understanding in detail reactivity and reaction mechanisms of those complex feedstocks still remains a challenge.

* Corresponding author.
E-mail address: thierry.gauthier@ifp.fr (T. Gauthier).

0920-5861/$ – see front matter © 2009 Elsevier B.V.. All rights reserved.
doi:10.1016/j.cattod.2009.10.002

Residues are composed of large hydrocarbon structures characterized by a high polydispersity in terms of size and chemical composition [6]. High boiling point fractions contain the so-called resins and asphaltenes fractions, generally defined with high polarity and aromaticity, combined with large contents of heteroatoms such as sulphur (S) and nitrogen (N), metals such as vanadium (V) and nickel (Ni) and functional groups [7,8]. Some metal compounds for example are known to be included in complex structures such as porphyrines [9].

The analysis of such complex compounds remains challenging. Molecular analytical techniques generally used for lighter fractions can no longer be applied (i.e. gas chromatography), or are generally not sufficient in separation power. To study and characterize these structures, a simplification at a preparative scale of the matrice can be preliminary considered [10]. One of the possibilities is to decrease the polydispersity according to the polarity by liquid chromatography into four fractions termed Saturates, Aromatics, Resins and Asphaltenes (SARA) [11,12]. The recovered fractions can then be further characterized by various analytical techniques such as the ^{13}C Nuclear Magnetic Resonance (NMR) or the Size Exclusion Chromatography (SEC) [13,14]. Some techniques like the Fourier Transformed Ion Cyclotron Resonance Mass Spectrometry (FT-ICR MS) may be very useful to describe in detail hydrocarbon structures found in residue feedstocks [15,16].

Regarding hydroconversion in ebullated beds and slurry reactors, most of the recent papers discussed reactor operation. McKnight et al. [17] emphasized the importance of gas hold-up in industrial ebullated bed reactors with respect to design aspects. A detailed modeling of hydroconversion inside the ebullated bed has been proposed by Schweitzer and Kressmann [18]. In this study, they consider an axial dispersion of liquids in reactor combined with a four lump approach for the cracking mechanisms with first order reactions. Recently, Gauthier et al. [19] studied further the ebullated bed process regarding operating condition effect on vacuum residue hydroconversion. This study focused on the importance of vaporization in a reactor in a bench unit consisting of two elongated reactors operating in ebullated bed mode. They concluded that vaporization has to be accounted for to model residue hydroconversion as a function of temperature and reaction time. Their data also suggest that hydroconversion can be adequately represented by an apparent second order kinetics.

The role of the catalyst during hydroconversion has been studied previously [20,21]. Miki et al. [20] showed that catalyst mainly hydrogenates heavy molecules into lighter cuts, transferring hydrogen to the radicals formed by thermal cracking. Gray et al. [21] added that another catalyst's role is to help heteroelement removal from the residue. Mosio-Mosiewski and Morawski [22] studied vacuum residue hydroconversion in a continuous flow reactor with dispersed catalyst as a function of operating conditions. This study confirmed that conversion is mainly dependent on temperature and reaction time, and almost irrespective on hydrogen pressure and catalyst concentration. The study was conducted for a given feed (Ural), but overall, there is little information on the feed reactivity as a function of its composition.

The yields and cracking reactions resulting from residue upgrading may be linked to feed composition. In the literature, most of the published studies focus on asphaltenes conversion. As an example, the evolution of the asphaltene structure in function of the conversion has been studied in some previous works [23,24] with the proposal of an average molecular representation of asphaltene evolution in hydroconversion conditions. But there is few information on the feed reactivity as a function of their composition. Nagaishi et al. [25] have studied hydroconversion mechanisms in a batch reactor with multipass operation. They showed that as the more reactive species are depleted, the first order rate constant for residue decreases with increasing conversion. Fukuyama and Terai [26] studied kinetics of hydrocracking reaction of vacuum residue using SARA constituents in the 525 °C$^+$ residue fraction and gas, naphtha, kerosene, gas oil, vacuum gas oil and coke as products. They showed that the catalyst used reduced polycondensation reactions. Shuyi et al. [27] studied the conversion of an atmospheric residue under severe conditions in the presence of a dispersed catalyst. They compared their results with those obtained with only thermal cracking under the same conditions. They showed that product selectivity is affected in the presence of a dispersed catalyst: residue conversion was limited while coke and light fractions such as gas and naphtha were reduced. This confirmed the stabilizing role of the catalyst.

The objective of the present study is to detail hydroconversion reaction mechanisms of the different chemical species composing the residue, in order to better describe feed reactivity effects. In a first step, physicochemical characterization has been performed on several vacuum residues from different geochemical origins exhibiting different macroscopic properties. Some of those feeds have already been tested in industrial development studies in the past and exhibited differences in reactivity in hydroconversion pilot plants. A detailed analytical characterization of each feed was conducted and led to the conclusion that reactivity may be related to SARA composition. Therefore, one feed was then selected (Athabasca bitumen) in order to investigate potential reactivity differences of SARA fractions which may then explain feed reactivity differences based on SARA composition. This feed was separated by polarity in different fractions at a preparative scale in order to later study hydroconversion of these different fractions. An autoclave batch reactor was adapted in order to study the reactivity of the initial residue feedstock and later on in a next step, the reactivity of the separated fractions prepared from the residue.

2. Experimental

2.1. Feedstocks analysis

Four vacuum residues of different geochemical origins have been analyzed in order to investigate their specific composition and properties: Athabasca (Canada), Ural (Russia), Duri (Indonesia) and Arabian Light (Middle East). Standard properties have been measured (d4/15, viscosity) and Elemental Analysis (EA) have been performed on the four selected vacuum residues (S, N, Ni, V, C, H contents) to globally characterize the residues.

Concerning the SARA separation, the deasphalting step is based on sample flocculation in contact with a paraffinic solvent. It is well known that parameters such as contact time, solvent/oil ratio, type of solvent, temperature and washing steps can strongly influence the precipitation [28]. For this study, precipitation of asphaltenes was performed through a derived method from the norm NF T60-115, using *n*-heptane at 80 °C with an oil/heptane ratio of 1/50 (v/v). In a second step, the SAR fractionation was conducted by liquid chromatography at an analytical scale.

The determination of the molecular weight of asphaltenes and to a lesser extent of resins is complex due to their high polydispersity, heterogeneity and tendency to form aggregates. The association state of these molecules is known to be very sensitive to experimental conditions such as concentration, temperature and solvent [29,30]. Due to these properties, the interpretation of analytical results may be tedious. It has been shown that the molecular weight of asphaltenes measured with different techniques can vary by several orders of magnitude since the asphaltenic structures are not measured in the same state [30].

In this study, the distribution of apparent molecular weight of residues and SARA fractions were estimated using Size Exclusion

Chromatography (SEC) since it can be routinely used. In case of asphaltene measurements, results may however be biased due to association and non-size effects [8,13]. SEC was performed on a WATERS Alliance 2695 using a refractive index detector. The system was controlled using an Empower chromatography manager. Calibration was performed using 10 monodisperse polystyrene standards with masses in the range of 162–120,000 g/mol (Polymer Laboratories). Samples were injected at a concentration of 5 g/L in tetrahydrofuran (THF) with a volume of 50 μL. The column temperature was fixed at 40 °C and the flow rate at 0.7 mL/min. Three columns packed with polystyrene-divinylbenzene supports (PS-DVB, Polymer Laboratories) were chosen. The corresponding porosities are 100, 1000, and 10,000 Å, and the column characteristics are as follows: particle size, d_p = 5 μm; column length, L = 300 mm; internal diameter, 8 mm. SEC data enables to describe the weight distributions, from which a weight average molecular weight M_w is calculated as follows:

$$M_w = \frac{\sum N_i M_i^2}{\sum N_i M_i} \quad (1)$$

where N_i represents the number of molecules of M_i molecular weight, in g/mol.

In order to further characterize their chemical structure as a function of conversion, asphaltene samples were also analyzed using ^{13}C Nuclear Magnetic Resonance (NMR). This technique enables to quantitatively characterize the various carbon types found in the samples. NMR experiments were performed on an Advanced 300 MHz Bruker spectrometer, using a 10 mm BBO ^1H/X/D NMR probe. The chemical shifts were referenced using $CDCl_3$ as the solvent. Samples were prepared by mixing 100 mg of fractions in 3 mL of $CDCl_3$ to obtain a homogeneous solution. ^{13}C NMR direct acquisition spectra were realized with a 60° flip angle at a radio frequency pulse of 20 kHz, which provided the quantity of saturated and unsaturated C atoms. In addition, two ^{13}C NMR experiments, based on the scalar coupling between proton and carbons, were conducted to obtain data about paraffinic, naphtenic, and aromatic carbon species. The spin-echo experiment allowed the aromatic and aliphatic carbon species to be quantified separately, and the Attached Proton Test (APT) series was applied to identify and quantify the proportion of C atoms, as a function of the number of proton in their neighborhood.

Based on this method, it was possible to determine the proportion of CH and quaternary C (C_q) present in the aromatic part and the proportion of CH_3, CH_2, CH and quaternary C (C_q) present in the aliphatic part. Using the amount of total aromatic carbon and the detailed %CH and %C_q, it is possible to calculate the substitution index I_s defined as the ratio between the substituted and the substitutable aromatic carbons. It is also possible to compute a condensation index I_c, which corresponds to the average number of aromatic cycles composing the structure using two ideal aromatic cycles arrangements (peri-condensed I_{cp} and cata-condensed I_{cc}, as shown in Fig. 1). The representation of peri- and cata-condensed rings can be illustrated by model molecules such as pyrene and naphthalene as shown in Fig. 1a and b, respectively. These indexes are represented by Eqs. (2)–(4):

$$I_S = \frac{C_{qsub}}{C_{aro} - C_{qcond}} \quad (2)$$

$$I_{cp} = \frac{1 + 2(C_{qcond}/C_{aro})}{1 - (3C_{qcond}/2C_{aro})} \quad (3)$$

$$I_{cc} = \frac{1 + \left(\frac{C_{qcond}}{C_{aro}}\right)}{1 - 2\left(\frac{C_{qcond}}{C_{aro}}\right)} \quad (4)$$

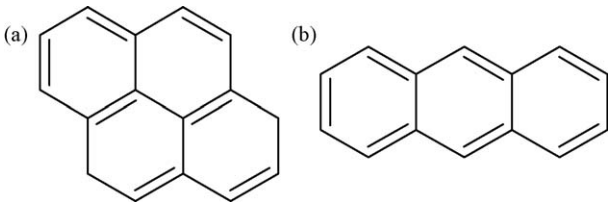

Fig. 1. Peri-condensed rings (a) and cata-condensed rings (b).

where C_{aro} corresponds to the total amount of aromatic carbons, C_{qsub} corresponds to the amount of quaternary aromatic carbons substituted by an aliphatic chain, and C_{qcond} corresponds to the amount of quaternary condensed aromatic carbons.

2.2. Separation of residue in different SARA fractions at a preparative scale

In order to study the reactivity of SARA fractions in a batch reactor, it is necessary to recover each SARA fraction at a preparative scale (kilogram scale). Since the analytical SARA technique currently used in liquid chromatography enables to recover only few hundred of milligrams of each fraction, an alternative separation method is required to prepare large amounts of residue fractions. The concept of consecutive deasphalting steps with different solvents is here used. Regarding such separation methods at the preparative scale, only few information is displayed in the literature. Only industrial patents showing the interest of combining consecutive deasphalting and deresining steps could be found [31–33].

In this study, we used a 60L deasphalting batch reactor. A dedicated protocol has been developed to optimize liquid–liquid separations operated in series with *n*-paraffinic solvents (Fig. 2). First of all, the vacuum residue is sent to the first step of deasphalting, in which the residue is intensively mixed with *n*-heptane at 220 °C. The mixture is then settled and two phases are recovered: (a) the residue fraction insoluble in the solvent (called Asphalt C7 fraction); and (b) the solvent and the soluble fraction of the residue (called DeAsphalted Oil or DAO C7 fraction). The solvent is then separated by distillation from the DAO C7. In order to improve the separation, this step is conducted two times, corresponding to the two stages in Fig. 2.

Then, this DAO C7 fraction is sent to the second step of deasphalting, in which it is intensively mixed this time with *n*-propane at 60 °C. The mixture is then settled. The two recovered phases are (c) the insoluble fraction in the solvent (called Resins C3 fraction) and (d) the solvent and the soluble portions of the DAO C7 (called DeAsphalted-deResined Oil or DARO C3 fraction). The solvent is then removed by distillation. This step is conducted three times, corresponding to the three stages in Fig. 2.

2.3. Reactivity experiments

The pilot plant designed for this study is an autoclave reactor, featuring a 300 mL total reactor volume. The pilot plant was designed to operate in batch mode, without liquid or gas circulation.

In order to limit pressure variations related to hydrogen consumption or gas formation, the amount of liquid feed in the autoclave is limited to 30–60 mL. The amount of hydrogen available in the gas phase is then large enough compared to the amount of hydrogen reacting which results in limited pressure variations during one test. Reaction time is depending upon exposure of the feed to the reaction temperature. Typical reaction times vary in the range of 1–4 h. Therefore, the autoclave was equipped with an internal furnace providing fast heating rates and a vortex cooling system to quench quickly the reaction.

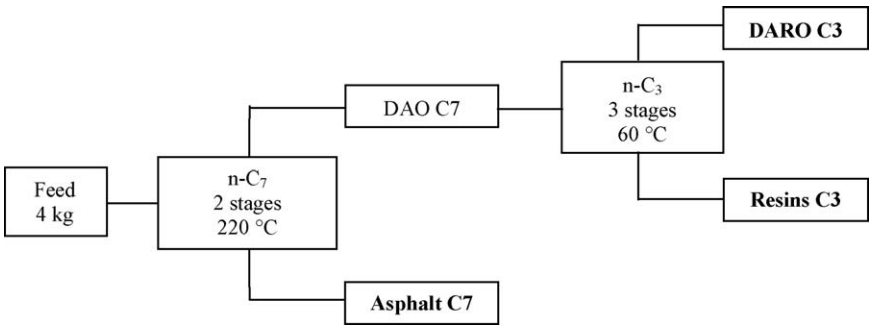

Fig. 2. Scheme of the protocol developed at a preparative scale (kg) to obtain SARA fractions: a two liquid–liquid separation operated in series with *n*-paraffinic solvents.

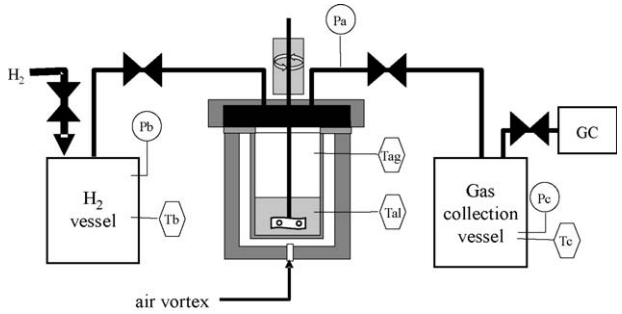

Fig. 3. Diagram of the batch reactor unit used for hydroconversion experiments.

The pilot plant is shown in Fig. 3. Liquid feed and catalyst are introduced in the autoclave before the test. Hydrogen is then introduced into the reactor at the beginning of the experiment from a hydrogen vessel. The autoclave furnace then heats up quickly the gas liquid mixture up to the reaction temperature for reaction start-up (less than 15 min from 100 to 420 °C). During reaction, temperature remains constant. No gas or liquid flows through the reactor and pressure variations only depend upon gas formation or consumption. When reaction time is over, the furnace is stopped and an air vortex provides a rapid temperature quench of the mixture below 350 °C, stopping therefore reactions (less than 15 min to cool from 420 to 100 °C). When reaction effluents reach ambient temperature, all gases are depressurized to a gas collection vessel (initially set up under vacuum conditions). Pressure variations of the gas collection vessel combined with GC analysis of the gas then enable to determine the gas amount and its composition at the end of the test. The liquid converted is then recovered.

Details on the evolution of the temperature and pressure during a typical test are illustrated in Fig. 4. The reactor is loaded with 50 g of feedstock and 0.45 g of crushed equilibrium industrial Ni–Mo catalyst. The liquid phase is stirred, favoring the liquid saturation in hydrogen and the catalyst suspension. The pressurization of the mixture with hydrogen in excess is adjusted at 110 °C in the autoclave to such a level to reach the desired pressure reaction at the reaction temperature. Gas phase is then preheated for 1 h. Liquid phase is then quickly heated at the reaction temperature. At the end of the reaction (after a few hours), the reactor is quickly cooled down with an air vortex system.

After reaction, at ambient conditions, gas effluents are directly transferred into a 5L vacuum vessel until pressure equilibrium between the vacuum vessel and the reactor is achieved. All gas and liquid products are therefore recovered, weighed and analyzed (gas losses when autoclave is open represents less than 1% of the gas remaining at the end of the test). Pressure and temperature data are measured during each step of the experiment. Fig. 4 shows a decrease of the pressure during the test: this evolution is related to hydrogen consumption during the test which is larger than the

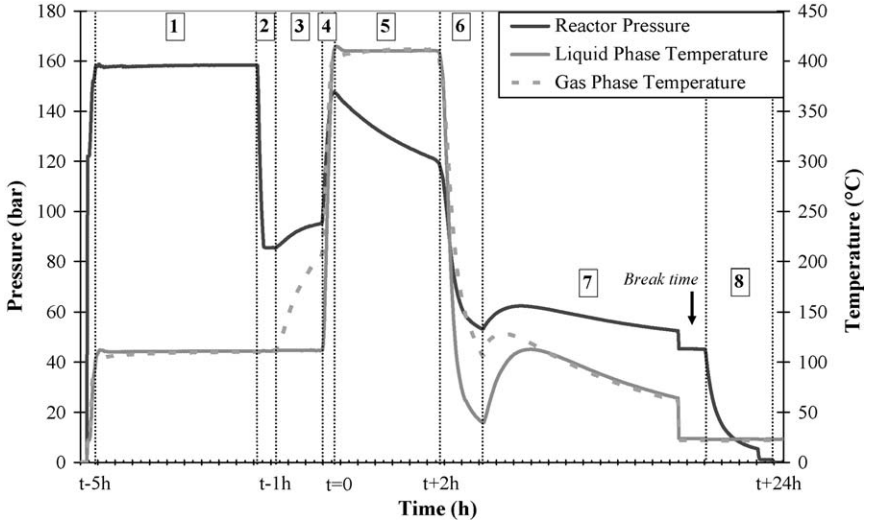

Fig. 4. Temperature and pressure evolutions in the reactor during a hydroconversion test. 1: Pressure test; 2: pressure adjustment at 110 °C to be at 150 bars at temperature test; 3: pre-heating gas phase; 4: heating liquid phase; 5: hydroconversion test; 6: cooling down gas and liquid phases with air vortex; 7: end of cooling down; 8: gas effluents transfer into the vacuum vessel.

amount of gas formed by hydroconversion. However, the final quantity of hydrogen still remains in large excess at the end of the reaction.

Complete mass balances are performed on each experiment, as shown in Eq. (5):

$$M_{efl} + M_{efg} = \alpha(M_f + M_c + M_{H_2}) \quad (5)$$

where M_f represents the mass of feed, M_c the mass of catalyst, M_{H_2} the mass of hydrogen initially introduced in the reactor; M_{efl} represents the mass of liquid effluent, weighed at the end of the reaction and M_{efg} the mass of gas effluent determined by gas chromatography. M_{H_2} and M_{efg} are determined using thermodynamic modeling based on pressure, volume and temperature and accounting for gas dissolution in liquids. The coefficient α is the mass balance closure coefficient which should be equal to 1 without losses. In our case, typical mass balances closure coefficients range from 96.5 to 98 wt.%.

In order to characterize the liquid effluent, a filtration is required to remove catalyst particles. For an easier recovery, a limited amount of toluene is therefore mixed with liquid effluents at the opening of the autoclave. The mixture is then filtrated in a glass microfiber filter under a low N_2 pressure. Toluene is then isolated from the filtrate by distillation at 150 °C. The mass balances of the filtration step range between 90 and 95 wt.%. IBP-150 °C cut is characterized by simulated distillation (gas chromatography) to quantify the added toluene and the light hydroconverted products. Simulated distillation is also conducted on the 150 °C$^+$ cut to quantify each standard cuts like naphtha (150–220 °C), gas oil (220–375 °C), vacuum gas oil (VGO: 375–520 °C) and vacuum residue (VR > 520 °C).

Yields are determined based on the amount of products measured for the various cuts, accounting for mass balance losses during reaction and during filtration-distillation.

Residue conversion defined on the 520 °C$^+$ unconverted products is described by the following Eq. (6):

$$X^{520\,^\circ C^+}(\text{wt.}\%) = \left[\frac{M_f x_f^{520\,^\circ C^+} - M_r}{M_f x_f^{520\,^\circ C^+}}\right] \times 100 \quad (6)$$

where M_f represents the mass of feed, M_r the mass of 520 °C$^+$ liquid effluent and x_f the weight fraction of 520 °C$^+$.

In residue hydroconversion processes, catalyst deactivation is used to occur due to coke and metals deposits on catalyst. Therefore, in a batch reactor, it is important to use equilibrium catalysts with steady state activity instead of fresh catalysts which would exhibit a non-representative very high initial activity [34,35]. The reaction time in batch reactor is effectively small when compared to the life time of industrial residue hydroconversion catalysts.

The selected catalyst is a Ni–Mo extrudate catalyst supported on alumina. It has been sampled at the end of an hydroconversion test performed on a large pilot plant operated in continuous in ebullated bed. The catalyst extrudate is crushed before the tests in order to reduce particle size to 10–100 μm. This makes suspension of the catalyst in liquid much easier, prevents attrition of the catalyst and may also improve internal diffusions limitations inside the catalyst.

In the present study, hydroconversion experiments are conducted on an Athabasca vacuum residue. Different levels of conversion have been obtained by varying reaction temperature from 395 up to 420 °C while reaction time (2 h) and initial pressure (150 bars) remain constants. In addition, experiments at 395 °C were also conducted without catalyst in order to study the impact of hydroconversion catalyst on conversion and yield structure and to evaluate thermal cracking performances. This experiment without catalyst was only conducted at low temperature to avoid liquid product stability issues and coke formation.

In a near future, similar experiments will be conducted on the Athabasca DAO C7, DARO C3 and Resins C3 vacuum residue fractions and on Asphalt C7 fluxed with LCO to study the impact of the SARA composition on conversion and yield structure.

3. Results

3.1. Feedstocks analysis

Table 1 shows detailed petroleum and structural analyses of the four selected vacuum residues (Athabasca, Ural, Duri and Arabian Light). Those feedstocks were selected specifically from different geochemical origins and they exhibit different macroscopic properties. Some of those feeds have already been tested in hydroconversion pilot plants before, showing differences in reactivity. Table 1 clearly shows that these feedstocks are really different: Athabasca residue presents difficult handling properties (high density, high viscosity) as well as high content of heteroelements, which may affect catalyst deactivation and product qualities; on the opposite, Duri vacuum residue presents the lowest density, viscosity, and heteroelement contents, despite an asphaltene content that is slightly higher than the Ural residue.

Based on the *H*/*C* atomic ratio, the Athabasca residue seems to present the higher aromaticity. Besides, SARA composition varies strongly from one feed to another. Athabasca residue is characterized by high resins and asphaltenes contents (42.1 and 14.1 wt.%, respectively). This is consistent with the low hydrogen content in the residue. On the other hand, Duri feed contains a high saturates content (21.0 wt.%) and a relatively low aromatics content (28.6 wt.%), which is consistent with the high hydrogen content found for the residue.

Concerning the molecular weights determined by SEC (Table 1), it must be reminded that these values are apparent masses given in equivalent polystyrene. Relative comparison indicates that Athabasca residue exhibits the higher average molecular weight (5778 g/mol) while those of Ural and Arabian Light residues are in the same range (2689 and 2966 g/mol, respectively).

Table 2 gathers the analytical characterization obtained for resin fractions of each residue. SEC chromatograms of resin from the different feedstocks are also shown in Fig. 5 and average molecular weights obtained are in the same range. The highest average molecular weight is obtained for Duri resins (5628 g/mol) while the lowest average molecular weight is obtained for Ural resins (2976 g/mol). It is interesting to note that despite their different origin and concentration in residue, resins exhibit very

Table 1
Detailed petroleum analysis on selected residues.

Feed	Athabasca	Ural	Duri	Arabian Light
Density at 15 °C	1.044	1.003	0.964	1.022
Viscosity at 100 °C (cSt)	14563	540	396	964
Sulfur (wt.%)	5.74	2.72	0.58	4.22
Nitrogen (ppm)	6275	5800	5934	4011
Ni + V (ppm)	431	220	76	125
Carbon (wt.%)	82.68	85.00	86.24	84.22
Hydrogen (wt.%)	9.86	10.60	11.39	10.34
H/C ratio	1.43	1.50	1.58	1.47
SARA distribution				
Saturates (wt.%)	6.8	11.7	21.0	11.6
Aromatics (wt.%)	31.2	46.1	28.6	48.6
Resins (wt.%)	42.1	36.1	36.8	31.3
Asphaltenes (wt.%)	14.1	4.6	5.7	7.7
Losses (wt.%)	5.8	1.5	7.9	0.8
(*Res*+*Aro*)/(*Sat* + *Asph*)	3.5	5.0	2.4	4.1
Molecular weight (SEC)				
M_w (g/mol in equivalent polystyrene)	5778	2689	4931	2966

Table 2
^{13}C NMR, SEC and elemental analysis of feedstocks resins.

Feed	Athabasca	Ural	Duri	Arabian Light
Molecular weight (SEC)				
M_w (g/mol in equivalent polystyrene)	4695	2976	5628	3609
^{13}C NMR				
C_{aro} tot (wt.%)	36.90	37.20	33.70	41.00
CH (wt.%)	29.27	33.87	29.67	31.71
C_q (wt.%)	70.73	66.13	70.33	68.29
C_{qsub} (wt.%)	39.30	35.75	34.42	37.80
C_{qcond} (wt.%)	31.44	30.38	35.91	30.24
Cali tot (wt.%)	63.10	62.80	66.30	59.00
CH_3 (wt.%)	20.13	18.15	13.57	22.20
CH_2 (wt.%)	59.59	65.29	72.85	58.31
CH (wt.%)	18.38	16.56	13.57	19.49
I_s	0.57	0.51	0.54	0.54
I_{cp}	3.1	2.9	3.7	3.0
I_{cc}	4.4	4.1	6.1	4.1

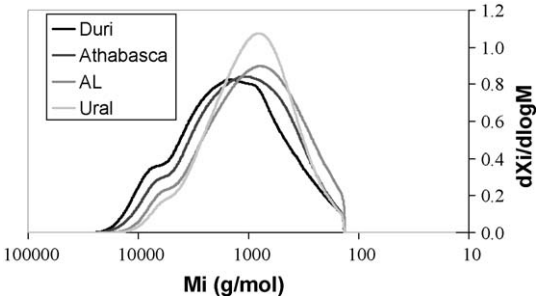

Fig. 5. SEC chromatograms of feedstocks resins.

similar average hydrocarbon structure, as measured through NMR. ^{13}C NMR results show that aromatic carbon content is relatively low, in a range from 33 to 41 wt.%. Duri feed exhibits a higher aliphatic CH_2 content than the others and a lower aliphatic CH_3 content, suggesting longer aliphatic chains. Similar results can be found on saturates and aromatics. However, such a conclusion can not be made with asphaltenes. The average molecular weight of asphaltenes determined by SEC changes significantly depending upon feed (from 6226 to 14738 g/mol) due to size effects, which is consistent with other published work [13].

As a consequence, results indicate that SAR fractions represent about 85–95 wt.% of the residue depending on the residue considered. In addition, for all residues studied, the SAR average hydrocarbon structure remains similar. Therefore, the main differences observed from one residue to another may be explained either by the differences in SAR repartition or by the asphaltene content and structure. This may explain differences of reactivity in hydroconversion from one feed to another that have already been observed before during previous hydroconversion testing. Since asphaltene concentration is rather small in residue, the feed effects on conversion and yields may be mostly related to differences in SAR repartition from one residue to another.

Based on all of these results, Athabasca vacuum residue has been selected for the subsequent experimentation for several reasons: (a) industrial interest (production increase in Alberta, Canada) and (b) the high content in resins and asphaltenes enables the easier recovery of significant quantities of the required fractions for batch experimentations.

3.2. Separation of residue in different SARA fractions at a preparative scale

The Athabasca residue has been separated in different fractions using successive liquid–liquid extractions with heptane and propane according to the protocol described earlier. SARA analysis (performed by analytical liquid chromatography) of the different fractions Asphalt C7, DAO C7, Resins C3 and DARO C3 are reported in Table 3. SARA mass balances are presented either as a repartition of the fraction itself (“compo” as composition in Table 3), or as a repartition relative to the feed (“select” as selectivity in Table 3). The latter information allows to estimate the repartition of the saturates, aromatics, resins or asphaltenes of the feed in each Asphalt C7, DAO C7, Resins C3 and DARO C3 fraction. Losses resulting from the analytical SARA analysis (generally less than 5%) have been considered as resins because of their irreversible adsorption on the chromatographic column.

Asphalt C7 represents about 25% of the residue and contains all asphaltenes from the residue, and 22 wt.% of the initial resins. Resins C3 represent 41% of the residue, contain most of the resins from the residue (62 wt.%) and a significant part of the aromatics (37 wt.%). The remaining DARO C3 contains all saturates from the residue and 62 wt.% of the aromatics.

These results highlight the lower selectivity of the protocol set up at a preparative scale when compared to the analytical SARA separation. The separation into fractions containing only asphaltenes, resins, aromatics or saturates respectively is not ideal. However, the Asphalt C7 contains most of the asphaltenes, the Resins C3 fraction is enriched in resins and the DARO C3 contains most of the saturates and aromatics, as confirmed by SARA compositions. In the future, those fractions will be converted in the same conditions than the residue in the autoclave reactor to study feed composition effect during hydroconversion.

3.3. Reactivity experiments

Fig. 6 shows 520 °C$^+$ conversion of the Athabasca residue as a function of temperature. As expected, conversion strongly increases when temperature increases, ranging from 34.2 wt.% at 395 °C up to 67.4 wt.% at 420 °C. With catalyst, conversion

Table 3
SARA composition of each family obtained after liquid–liquid fractionation.

			n-C_7 deasphalting				*n*-C_3 deresining			
	Athabasca VR		Asphalt C7		DAO C7		Resins C3		DARO C3	
Yield (wt.%)	100.0		24.8		75.2		41.4		33.8	
	SARA compo[a]	*SARA select*	SARA compo[a]	*SARA select*	SARA compo[a]	*SARA select*	SARA compo[a]	*SARA select*	SARA compo[a]	*SARA select*
S (wt.%)	7	*100*	0	*0*	9	*100*	0	*0*	20	*100*
A (wt.%)	31	*100*	1	*1*	41	*99*	28	*37*	58	*62*
R (wt.%)	48	*100*	42	*22*	50	*78*	72	*62*	22	*16*
As (wt.%)	14	*100*	57	*100*	0	*0*	0	*0*	0	*0*

“Compo”, as composition, represents the SARA repartition of the fraction itself; “select”, as selectivity, represents the SARA repartition relative to the feed.
[a] Normalized SARA.

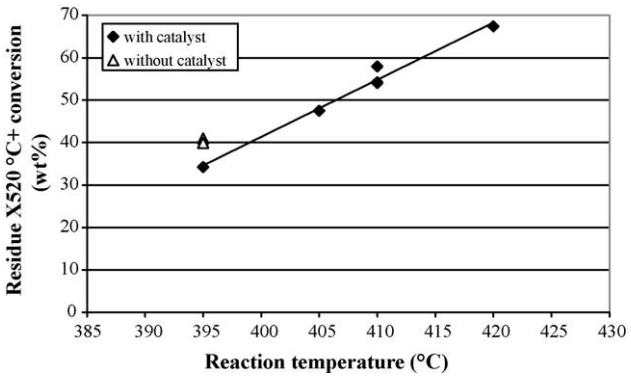

Fig. 6. Residue 520 °C$^+$ conversion as a function of temperature.

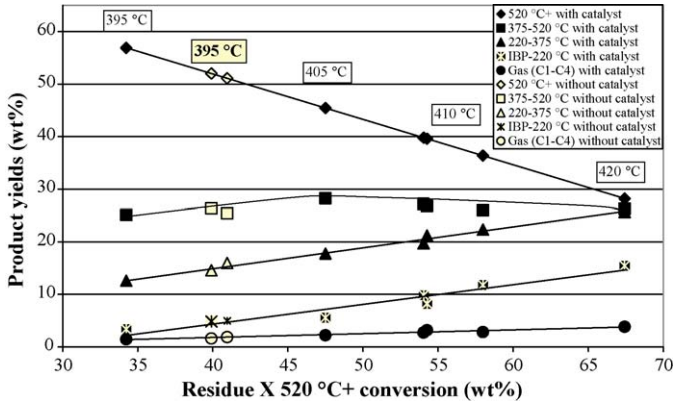

Fig. 8. Product yields selectivity as a function of residue conversion.

increases quite linearly with temperature. This trend is consistent with expectations, since conversion follows an apparent second order kinetics versus residue concentration [19]. Such results do suggest an activation energy in the range of 217 kJ.mol^{-1}, consistent with large-scale pilot plant units operating in similar conditions.

An additional experiment was conducted at 410 °C with increasing reaction time. In those conditions, a conversion of 64 wt.% was found suggesting an apparent second order. Indeed, with an order of one, higher conversion in the range of 67–68 wt.% should have been found. This is consistent with results obtained in a previous study where an apparent second order kinetics was already found [19] based on results obtained in a large-scale ebullated bed reactor. Our present result therefore tends to confirm the trends observed previously. This is not surprising. In the past, Ho and Aris [36] suggested that apparent second order reactions can arise when a reacting lump is composed of several species of different reactivity. As the more reactive species are depleted, the first order constant will decrease with increasing conversion [25]. As several parallel first order reactions probably occur during hydroconversion, the conversion can be represented globally by an apparent second order kinetics.

Surprisingly, for the same reaction time and temperature, conversion level is found higher without catalyst than with catalyst. The difference is in the range of 5 wt.% conversion. Similar trends are reported in the literature at several temperatures and lower hydrogen pressures [27,37]. Thermal cracking reactions may therefore be faster when no catalyst is present to stabilize radicals by catalytic hydrogenation. Del Bianco et al. [37] assumed that this type of catalyst has no effect on C–C bond cracking. Therefore, the quantity of free radicals is determined by the severity of the reaction.

Fig. 7 represents hydrogen consumption and C1–C4 gas yield as a function of 520 °C$^+$ residue conversion level. With catalyst, hydrogen consumption and gas formation both increase with the conversion of the residue, as expected.

Hydrogen consumption ranges from 0.7 to 1.5 wt.% when conversion increases from 34.2 to 67.4 wt.%. At these conversion levels, more radicals are formed and therefore more hydrogenation is required. Furthermore, desulphurization increases. Without catalyst, less hydrogen is, as expected, consumed, emphasizing the importance of catalyst for hydrogenation and hydrodesulphurization reactions.

When plotted as a function of residue conversion, C1–C4 gas formation increases similarly with conversion, with or without catalyst. This suggests that catalyst does not affect cracking reaction mechanisms. However, one has to keep in mind that, for a given temperature, gas formation will be higher without catalyst than with catalyst, since conversion is higher without catalyst. This is in agreement with previous studies which reported that gas formation is noncatalytic, whatever the temperature and residence time conditions [27,38].

Fig. 8 shows yield with standard cut points resulting from product analysis as a function of the 520 °C$^+$ residue conversion. As shown in Fig. 7 for C1–C4 cracked gases, all yields vary similarly as a function of conversion with or without catalyst. IBP-220 °C yield increases with conversion: naphtha yield varies from 3.4 to 15.5 wt.% while residue conversions vary from 34.2 to 67.4 wt.%. 220–375 °C cut follows the same trend as it raises from 12.6 up to 25.7 wt.%. 375–520 °C cut initially slightly increases until to reach a maximum of 28.0 wt.% at 47.5 wt.% residue conversion before decreasing. 375–520 °C VGO is an intermediate product that results on one hand from residue cracking but on the other hand can probably also crack into lighter products. 520 °C$^+$ yield

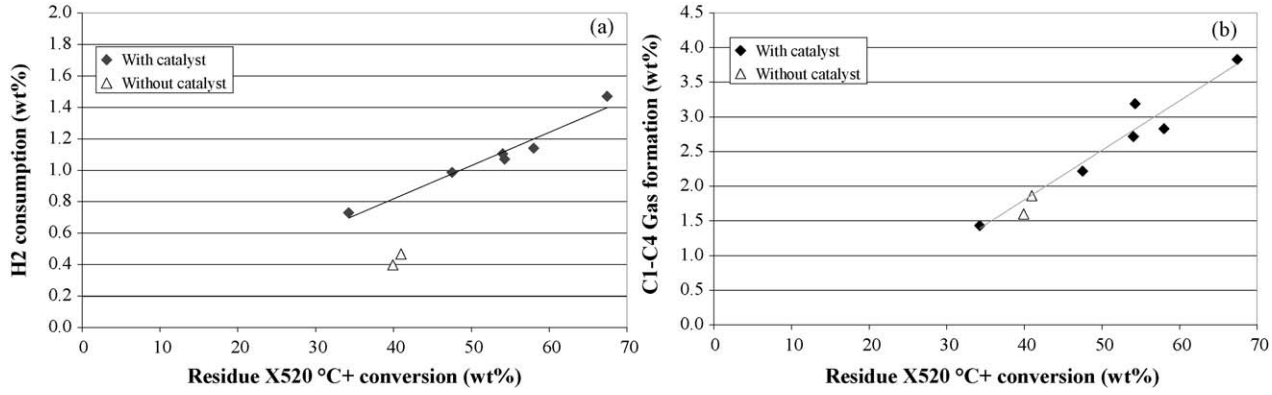

Fig. 7. Hydrogen consumption (a) and C1–C4 gas formation (b) as a function of residue conversion.

Table 4
Product yield selectivity as a function of residue conversion for experiments performed at 395 °C, in wt.% of the effluent.

Cut	Experiment performed with catalyst	Experiments performed without catalyst	
Gas/C1-C4	1.4	1.9	1.6
Naphtha/IBP-220 °C	3.4	5.0	4.9
Gas Oil/220-375 °C	12.6	16.0	14.6
Vacuum Gas Oil/ 375–520 °C	25.1	25.4	26.4
Vacuum Residue/ 520 °C$^+$	56.9	51.1	52.0

obviously decreases as a function of residue conversion. Thus, residue cracking reaction scheme may be described as follows: VR is first cracked into lighter cuts such as gas, naphtha, gas oil and VGO. Part of lighter cuts such as VGO can also crack to create lighter products. When residue conversion is high, VGO yield decreases, suggesting that VGO cracking is larger than VGO formation resulting from residue cracking. Fukuyama and Terai [26] showed this trend in a kinetic study of hydrocracking reaction of vacuum residue where they obtained maximum VGO yield at about 58 wt.% of the 525 °C$^+$ residue conversion.

Catalyst effects on yields as a function of conversion seem negligible which confirms the trend observed with C1-C4 gases. This supports that catalyst does not affect the cracking reaction mechanisms. Miki et al. [20] indicated that thermal cracking is the main route to form lighter fractions, observing the same results with or without catalyst. Gray et al. [21] showed the same trend using a Ni/Mo on γ-alumina catalyst. However, for the same conversion level, temperature is higher with catalyst than without catalyst. Therefore, when comparing product yields obtained with and without catalyst at the same temperature (395 °C, see Table 4), differences in yield structures can be found with and without catalyst. More residues are found with catalyst and less gas oil, naphtha and gases, consistently with Shuyi et al. [27]. At higher temperature, continuous operation without catalyst may however become difficult due to product stability issues. Without catalyst, polycondensation of aromatics is favored due to hydrogenation limitations and can result in coke formation at increasing severity.

Fig. 9 shows hydrodesulphurization performances in function of the VR conversion. As expected, hydrodesulphurization reactions increase with conversion, ranging in our case from 26 up to 47 wt.%. Hydrodesulphurization rate is probably depending upon catalyst concentration in the reactor, as suggested by the experiments from Mosio-Mosiewski and Morawski [22], removing sulphur as H_2S [20–22]. Hydrodesulphurization rate strongly decreases without catalysts since this reaction is mostly catalytic, while cracking reactions are mostly thermally controlled. Part of hydrodesulphurization is, however, resulting from cracking since hydrodesulphurization rate is not reduced to zero without catalyst. Sulphur bridges in molecules may therefore be weak points where cracking may occur thermally.

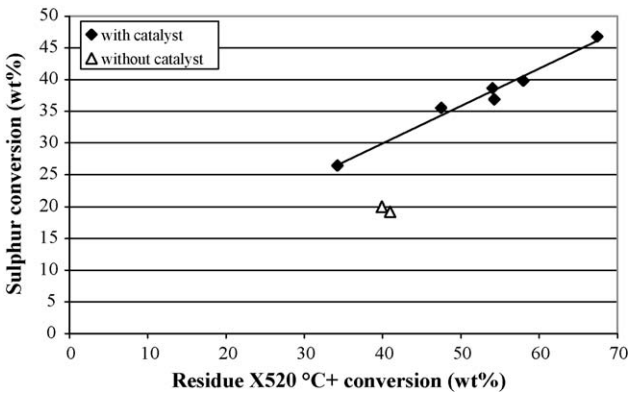

Fig. 9. Hydrodesulphurization as a function of residue conversion.

Future work will include similar experiments on Asphalt C7, DAO C7, Resins C3 and DARO C3 prepared from the Athabasca residue. Reactions rates, product yields and detailed analysis will be determined and compared to results obtained with the Athabasca feedstock in order to evaluate the impact of feed composition on hydroconversion mechanisms.

4. Conclusions

In this paper, a methodology is proposed to study hydroconversion mechanisms.

Detailed analyses of several residues show that the chemical composition of a feed strongly depends on its geochemical origin. From one residue to another, SARA composition varies significantly but, apart from the asphaltenes, the structural analyses of the different SAR fractions remain very similar. Therefore, SARA composition may directly be related to the hydroconversion reactivity of each residue.

A liquid–liquid extraction method was used to produce at the preparative scale (kg) fractions of Athabasca residue with different SARA compositions. By combining two successive liquid–liquid extractions (with heptane and propane respectively), it was possible to recover three fractions respectively enriched in asphaltenes, resins and aromatics + saturates.

A pilot plant was designed in order to conduct hydroconversion reactions with small feedstock quantities in batch mode. From this batch pilot plant operation, it is possible, thanks to complete mass balances and product analyses done for each test, to determine hydroconversion performances, yield structure, hydrogen consumption and some product properties depending upon the amount of products available.

Experiments were conducted on the whole Athabasca residue feed over a large temperature range resulting in a wide range of hydroconversion levels, with and without catalyst. The yield structure was determined and only seems to be related to hydroconversion level. Surprisingly, similar yield structures were found with and without catalyst. This supports the hypothesis that cracking mechanisms are thermally initiated. The presence of catalyst modifies however reaction rates, since different conversion levels were found at the same temperature. The catalyst only favors product hydrogenation and HDS reactions.

In a next step, the different residue fractions prepared by liquid–liquid extraction will be hydroconverted in similar operating conditions in order to compare reaction rates and yield structures obtained so as to determine the effect of feed composition on residue conversion.

Acknowledgments

The authors would like to acknowledge Jan Verstraete and Serge Coatanéa for their contribution, help and advice to this work.

References

[1] J.F. Le Page, S.G. Chatila, M. Davidson, Residue and Heavy Oil Processing, Editions Technip, Paris, 1992.
[2] M.R. Gray, Upgrading Petroleum Residues and Heavy Oils, Marcel-Dekker, 1994.
[3] M.S. Rana, V. Samano, J. Ancheyta, J.A.I. Diaz, Fuel 86 (2007) 1216.
[4] J.J. Colyar, L.I. Wisdom, in: Proceedings of the National Petroleum Refiners Association Annual Meeting, San Antonio, Texas, 1997.
[5] J.E. Duddy, L.I. Wisdom, S. Kressmann, T. Gauthier, in: Proceedings of the Third Bottom of the Barrel Technology Conference (BBTC), Antwerp, Belgium, 2004.

[6] E.Y. Sheu, Energy Fuels 16 (2002) 74.
[7] J. Murgich, J.M. Rodriguez, Y. Aray, Energy Fuels 10 (1996) 68.
[8] O.P. Strausz, P. Peng, J. Murgich, Energy Fuels 16 (2002) 809.
[9] O.P. Strausz, E.M. Lown, The Chemistry of Alberta Oil Sands Bitumens and Heavy Oils, Editions AERI, Canada, 2003.
[10] I. Merdrignac, D. Espinat, Oil Gas Sci. Technol. 62 (2007) 7.
[11] S. Peramanu, B.B. Pruden, P. Rahimi, Ind. Eng. Chem. Res. 38 (1999) 3121.
[12] L. Carbognani, A. Izquierdo, Preparative and automated compound class separation of Venezuelan vacuum residua by high-performance liquid chromatography, 1989.
[13] I. Merdrignac, C. Truchy, E. Robert, I. Guibard, S.P. Kressmann, Petrol. Sci. Technol. 22 (2004) 1003.
[14] M. Domin, A. Herod, R. Kandiyoti, J.W. Larsen, M.J. Lazaro, S. Li, P. Rahimi, Energy Fuels 13 (1999) 552.
[15] D.F. Smith, G.C. Klein, A.T. Yen, M.P. Squicciarini, R.P. Rodgers, A.G. Marshall, Energy Fuels 22 (2008) 3112.
[16] A.G. Marshall, R.P. Rodgers, Acc. Chem. Res. 37 (2004) 53.
[17] C.A. McKnight, L.P. Hackman, J.R. Grace, A. Macchi, D. Kiel, J. Tyler, Can. J. Chem. Eng. 81 (2003) 338.
[18] J.M. Schweitzer, S. Kressmann, Chem. Eng. Sci. 59 (2004) 5637.
[19] T. Gauthier, J.P. Heraud, S. Kressmann, J. Verstraete, Chem. Eng. Sci. 62 (2007) 5409.
[20] Y. Miki, S. Yamadaya, M. Oba, Y. Sugimoto, J. Catal. 83 (1983) 371.
[21] M.R. Gray, F. Khorasheh, S. Wanke, U. Achia, A. Krzywicki, E.C. Sanford, O. Sy, M. Ternan, Energy Fuels 6 (1992) 478.
[22] J. Mosio-Mosiewski, I. Morawski, Appl. Catal. A: Gen. 283 (2005) 147.
[23] I. Merdrignac, A.A. Quoineaud, T. Gauthier, Energy Fuels 20 (2006) 2028.
[24] T. Gauthier, P. Danial-Fortain, I. Merdrignac, I. Guibard, A.A. Quoineaud, Catal. Today 130 (2008) 429.
[25] H. Nagaishi, E.W. Chan, E.C. Sanford, M.R. Gray, Energy Fuels 11 (1997) 402.
[26] H. Fukuyama, S. Terai, Petrol. Sci. Technol. 25 (2007) 277.
[27] Z. Shuyi, W. Deng, H. Luo, D. Liu, G. Que, Energy Fuels 22 (2008) 3583.
[28] J.G. Speight, J. Petrol. Sci. Eng. 22 (1999) 3.
[29] B.P. Tissot, Rev. Inst. Fran. Petrol. 36 (1981) 429.
[30] J.G. Speight, D.L. Wernick, K.A. Gould, R.E. Overfield, B.M.L. Rao, D.W. Savage, Rev. Inst. Fran. Petrol. 40 (1985) 51.
[31] C.H. Watkins, Desulfurization of asphaltene-containing hydrocarbonaceous black oils, Universal Oil Products Company, US 3,775,293, Arlington Hgts., Illinois (1973).
[32] R.E. Leonard, Supercritical process for producing deasphalted demetallized and deresined oils. Kerr-McGee Refining Corporation, US 4,290,880, Oklahoma City, Oklahoma, 1981.
[33] J.J. Kolstad, Process for deasphalting resid, recovering oils, removing fines from decanted oil and apparatus therefore. Amoco Corporation, US 5,124,025, Chicago, Illinois, 1992.
[34] E. Furimsky, F.E. Massoth, Catal. Today 52 (1999) 381.
[35] B.M. Vogelaar, J. Gast, E.M. Douma, A.D. Van Langeveld, J.A. Moulijn, Ind. Eng. Chem. Res. 46 (2007) 421.
[36] T.C. Ho, R. Aris, AIChE J. 33 (1987) 1050.
[37] A. Del Bianco, N. Panariti, S. Di Carlo, P.L. Beltrame, P. Carniti, Energy Fuels 8 (1994) 593.
[38] F. Khorasheh, H.A. Rangwala, M.R. Gray, I.G. Dalla Lana, Energy Fuels 3 (1989) 716.